SINET: Ethiop. J. Sci., 41(2):46–52, 2018 ISSN: 0379–2897 (PRINT)

ISSN: 0379–2897

THERMOLUMINESCENCE FROM SILICON QUANTUM DOTS USING THE MODEL OF INTERACTIVE MULTIPLE TRAPS SYSTEM

Asamin Regassa and Belayneh Mesfin*

Department of Physics, Addis Ababa University, Addis Ababa, Ethiopia
E-mail: belayneh.mesfin@aau.edu.et

ABSTRACT: The effect of size variation on the intensity of thermoluminescence emission from spherical amorphous silicon quantum dots is investigated using the interactive multiple traps system model. The model consists of an active electron trap, a thermally disconnected deep trap, and a recombination center. Numerical simulations are carried out for quantum dots of diameters $3,4,5,6\,nm$ to determine the thermoluminescence glow curve and relevant important kinetic parameters. It is found out that as the size of the quantum dots decrease, the intensity of the thermoluminescence signal increase, the peak temperatures almost remains constant independent of the size of the dots, and the glow curve seems to obey first-order kinetics. In addition, the symmetry factor, the order of kinetics as well as the instantaneous concentration of carriers in the traps and recombination center are numerically simulated. The results obtained may be used while fabricating dielectric compounds enriched with silicon contents for TL applications.

Key words/phrases: Glow curve; Kinetic model; Quantum dot; Recombination coefficient; Thermoluminescence

INTRODUCTION

Thermoluminescence (TL) is the emission of light from an insulator or a semiconductor when it is heated following the previous absorption of energy from radiation (Mckeever, 1983; Furetta, 2003). A plot of the light intensity as a function of temperature is known as the glow curve. The luminescence of different silicon-based materials, such as hydrogenated amorphous silicon (a-Si:H) and silicon oxide (SiO_2), has been known for a long time (Rodriguez *et al*., 2014). Indeed, dielectric compounds enriched in different ways with silicon content, such as silicon-oxide or silicon-nitride have been found to be the most promising materials as light emitting devices (Rodriguez *et al*., 2014; Cabanas-Tay *et al*., 2016; Tu *et al*., 2012; Park et el., 2001).

Because silicon is an indirect-gap semiconductor, phonon-assisted radiative recombination is very inefficient and as its energy gap is small ($\sim 1.1eV$ for bulk) emission in the visible spectral region is precluded (Rodriguez *et al*., 2014). A different scenario is encountered when the particles dimensions are reduced to a few nanometres that is less than the size of the free exciton Bohr radius, i.e., $4.3nm$ in bulk Si (Rahdar *et al*., 2012; Yoffe, 1993). For such dimensions, the quantum size effect takes place resulting to the formation of discrete electronic levels, increased effective band gap, and oscillation strength as well as a considerable increase of radiative lifetime from a millisecond to a nanosecond (Rodriguez *et al*., 2014; Takagahara and Takeda, 1992). In particular, as a consequence of the quantum confinement effect compounded with its structural disorder and wide band gap energy ($\sim 1.6eV$ for bulk), amorphous silicon (a-Si) quantum dots has been found to be more efficient luminescence materials than crystalline silicon enabling it to be a viable candidate for short wavelength light emitters (Kwach *et al*., 2003; Park *et al*., 2001).

Different types of theoretical models have been proposed to describe the TL phenomena. The simplest and most commonly used TL model is the one trap and one recombination center (OTOR) model. Generally, the OTOR model may adequately describe almost all the basic TL characteristics, including the shape of the glow curve as functions of the heating rate and irradiation dose. However, a more detailed and accurate description of a TL phenomenon that agrees with experimentally observed TL glow curves requires a relatively more complex TL kinetic models, which take into account

*Author to whom correspondence should be addressed.

of multiple electron traps and luminescent centers (Pagonis and Kitis, 2012; Pagonis *et al*., 2006). Typical representatives of such models are the interactive multiple traps system (IMTS) and non-interactive multiple traps system (NMTS). Besides the active electron (dosimetric) traps, these models are characterized by the presence of thermally disconnected deep (competitor) traps.

An extension of the OTOR model is the two (three) active electron traps and a recombination center (TTOR) model. Using the TTOR kinetic model, Nebiyu *et al*. have studied the effect of size and retrapping on the intensity of TL emission in small a-Si quantum dots of diameters between $2-8nm$ (Nebiyu *et al*., 2017; Nebiyu *et al*., 2016). Their analysis shows that the TL glow curve possesses two (three) peaks corresponding to the two (three) active electron trapping levels, the TL intensity increases with a decrease in the size of quantum dots (QDs), and the simulated glow peaks corresponding to each trap levels obey second-order kinetics. Here, we find it interesting to further investigate the effect of size variation on the shape of the glow curve and TL intensity from silicon QDs by using thermally disconnected deep traps (TDDT) into the OTOR model.

Accordingly, we investigated the dependence of the intensity of TL emission and shape of the glow curves on the size of a-Si QDs using the IMTS kinetics model which consists of a dosimetric trap, a competitor trap, and a recombination center. Employing this model numerical simulations are carried out to determine the TL intensity, the symmetry factor, order of kinetics, and the instantaneous concentration of carriers in the electron traps, conduction band, and recombination center. The paper is organized as follows: The TL kinetic model and the rate equations that describe the traffic of carriers in the system are presented in the second Section. In the third Section, the numerical simulations and results are discussed. Finally, concluding remarks are given in the last Section.

MATERIALS AND METHOD

The IMTS model

In our investigation, we used the IMTS TL kinetic model, shown schematically in Figure 1. It consists of two electron trapping states and a recombination center (RC). The active electron trap (AT) is considered to be the one responsible for the TL signal, while the second deep electron trap (TDDT) is considered to be thermally disconnected, so that there is no thermal excitation of these electrons into the conduction band.

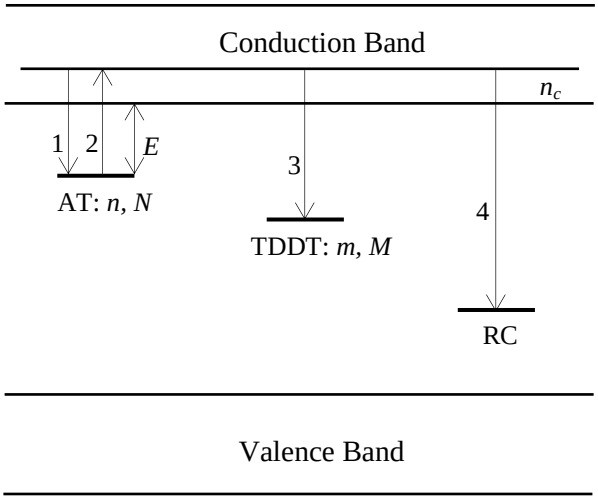

Figure 1: The IMTS model having an active electron trap (AT), a thermally disconnected deep electron trap (TDDT), and a recombination center (RC). The upward/downward directed arrows indicate the possible electron transitions during TL read-out.

In Figure 1, it is assumed that the process of traps/centers filling is already attained with priori irradiations of the sample by ionizing radiations. During trap emptying, electrons trapped in AT may be released from it (transition 2) by thermal stimulation of energy comparable to the activation energy, E, of the trap. Subsequently, these thermally elevated free electrons are released back from the conduction band either to recombine with the holes in the RC (transition 4) yielding luminescence, or end up being retrapped in the TDDT or AT (transitions 1 and 3).

For the proposed IMTS model, the transport of carriers during heating can be described by the following TL kinetic rate equations (Pagonis and Kitis, 2012; Sunta, 2015):

$$\frac{dn}{dt} = -sne^{-E/kT} + (N-n)n_c A_n, \quad (1)$$

$$\frac{dm}{dt} = (M-m)n_c A_m, \quad (2)$$

$$\frac{dn_h}{dt} = \frac{dn}{dt} + \frac{dm}{dt} + \frac{dn_c}{dt}, \quad (3)$$

$$\frac{dn_c}{dt} = -\frac{dn}{dt} - \frac{dm}{dt} - n_c n_h A_h, \quad (4)$$

$$I(t) = -\frac{dn_h}{dt} = n_c n_h A_h, \quad (5)$$

where $I(cm^{-3}s^{-1})$ is the intensity of the glow curve, N and M (cm^{-3}) are the total concentrations of the active and TDDT electron traps, n and m (cm^{-3}) are the corresponding instantaneous concentrations of filled traps, n_c (cm^{-3}) is the instantaneous concentration of electrons in the conduction band, n_h (cm^{-3}) is the concentration of carriers in the recombination center, A_n and A_m (cm^3s^{-1}) are the capture coefficients for the active and TDDT electron traps, A_h (cm^3s^{-1}) is the capture coefficient of the recombination center, $E(eV)$ is the activation energy of the active trap, $s(s^{-1})$ is the frequency factors for the active trap, and $k(eV/K)$ is the Boltzmann's constant. The initial concentrations of the dosimetric and competitor traps at time $t=0$ are denoted by n_0 and m_0, respectively. Moreover, we assume a linear heating given by

$$T(t) = T_0 + \beta t. \quad (6)$$

where $T(K)$ is the temperature of the sample at time t, $\beta(Ks^{-1})$ is the heating rate, $t(s)$ is the time, and T_0 is the temperature at $t=0$.

Because of the conservation of charge in the crystal, the concentration of holes, n_h, in the RC at any moment must be equal to the total instantaneous concentration of electrons (Pagonis *et al*., 2006). That is,

$$n_h = n + m + n_c. \quad (7)$$

Equations (1) - (5) are coupled nonlinear first-order differential equations, which generally do not have exact analytical solutions. The development of analytical expressions for the TL intensity requires simplifying assumptions like the quasi-equilibrium conditions, which for the IMTS model considered here are given by $n_c >> n$, m and $dn_c/dt >> dn/dt, dm/dt$. In our case, we make numerical simulations of the various parameters of interest using the MATHEMATICA9.0 software.

It is worthwhile to note that, for the case $M = m_0 = 0$, the IMTS model becomes the OTOR model. In order to make comparison between IMTS and OTOR, the TL intensities are calculated using both models.

Usually a TL glow curve is characterized by its symmetry factor (μ_g) defined as $\mu_g = \delta/\omega$, where $\delta = T_2 - T_m$ is the half-width toward the fall-off side of the glow peak, $\omega = T_2 - T_1$ is the full width at half maxima, T_m is the peak temperature, T_1 and T_2 $(T_2 > T_1)$ are the temperatures on either side of T_m, corresponding to half intensity. The values $\mu_g = 0.42$ and $\mu_g = 0.52$ correspond to first-order and second-order TL glow peaks, respectively. Moreover, μ_g is related to the order of kinetics, b, by the following empirical quadratic equation (Karmakar *et al*., 2017; Singh *et al*., 2012):

$$\mu_g = 0.25 + 0.186b + 0.024b^2. \quad (8)$$

For a particular value of μ_g, Eq. (8) may be solved to obtain the corresponding value of b.

RESULTS AND DISCUSSION

For numerical evaluations, we used the values $A_n = A_m = 10^{-9}\, cm^3s^{-1}$ for all QDs sizes neglecting any possible corrections associated with confinement. In addition, the size-dependent recombination coefficients defined by $A_h = \gamma/n_h$, where γ is the electron-hole radiative recombination rates are determined from the values displayed in Table 1.

Table 1. Size dependent radiative recombination rates of a-Si QDs (Abdul-Ameer & Abdulrida, 2011)

Radii of the QDs (nm)	$\gamma(s^{-1})$
1.5	7.0 x 10^6
2.0	3.0 x 10^6
2.5	9.0 x 10^5
3.0	4.0 x 10^5

Figure 2 shows the variation of concentrations of trapped electrons $n(T)$ in the active electron trap (AT) as a function of temperature. The concentration of electrons in the trap initially remains constant up to a temperature of about $T \approx 70\,^0C$, indicating that the trap is not yet activated. Thereafter, $n(T)$ decreases as the temperature increases until it is completely

emptied just above $180\,^0C$. Moreover, it is seen that $n(T)$ is almost independent on the size of the QDs.

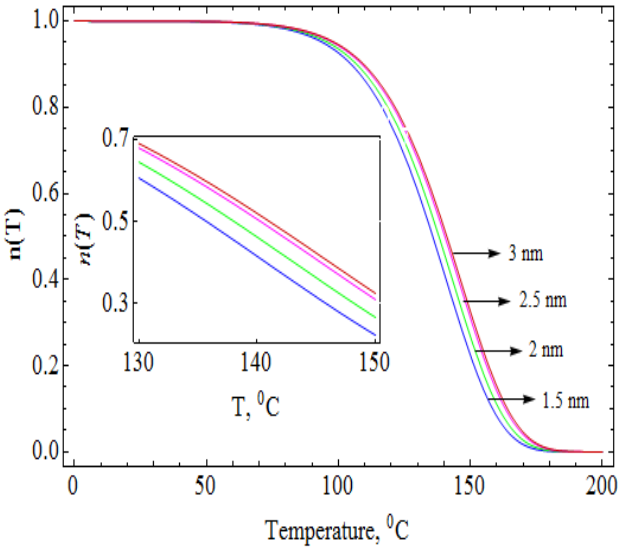

Figure 2: The normalized concentration of trapped electrons in the trap AT as a function of temperature for QDs of radii ranging between $1.5-3nm$. The values used for the simulation are: $A_n = A_m = 10^{-9}\,cm^3 s^{-1}$, $N = M = 10^{16}\,cm^{-3}$, $n_0 = m_0 = 2\times10^{14}\,cm^{-3}$, $\beta = 1Ks^{-1}$, $E = 0.75eV$, and $s = 10^8\,s^{-1}$.

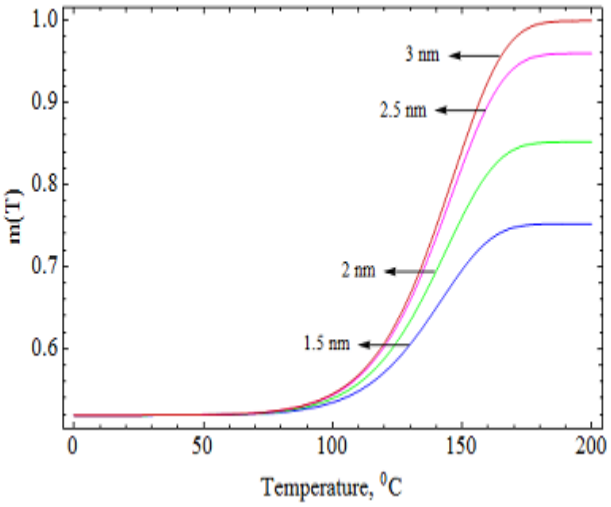

Figure 3: The normalized concentration of trapped electrons in the thermally disconnected deep trap (TDDT) as a function of temperature for different QDs size. The parameters are the same as in Figure 2.

Figure 3 depicts that for all the QDs, the instantaneous concentration of electrons $m(T)$ in the TDDT electron traps increases with an increase in temperature until about $180\,^0C$ and then reach saturation values just after about $180\,^0C$. The temperature $\sim 180\,^0C$ at which $m(T)$ becomes saturated also corresponds to the value where the TL glow curves ends (see Figure 5). Moreover, the saturation values are seen to increase with an increase in the size of the QDs. This may be explained in terms of the difference in the recombination coefficients, A_h, i.e., as the size of the QDs increases, A_h decreases which in turn means lesser number of electrons from the active electron trap reaching the RC and producing TL emission; instead many more electrons are more likely to be retrapped in the TDDTs before reaching the RC.

The variation of concentrations of electrons $n_c(T)$ in the conduction band as a function of temperature is shown in Figure 4 for the QDs of radii between $1.5-3nm$. It is seen that when the quantum dots sizes increase, $n_c(T)$ also increase. It is because that the recombination lifetime, which is the mean time spent by an electron in the conduction band, is large for larger QDs than the smaller ones. It means that free electrons in the conduction band spend more time before recombining with the holes in the RC in QDs with larger size than those with small size. In other words, A_h represents the recombination transition coefficient for electrons in the conduction band to recombine with holes in the luminescent centers and hence small A_h (larger QD size) means slow rate of recombination with the holes as the electrons spend more time in the conduction band.

It is worthwhile to note that unlike experimental techniques in which only the TL glow curves are generated, the numerical (theoretical) method enables us to observe how the concentration of carriers in the system evolve with the variation of QDs size and temperature.

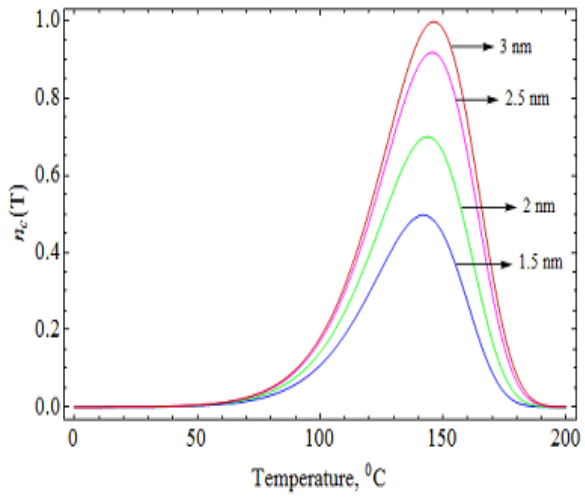

Figure 4: The normalized instantaneous concentration of free electrons in the conduction band as a function of temperature for different QDs sizes. The parameters are the same as in Figure 2.

Figure 5 depicts the intensity of the TL signal as a function of temperature. It shows that as the quantum dots size decreases, the intensity of the TL emission increases. The enhancement the TL signal with a decrease in QDs size may be explained with the fact that the intensity of TL emission from quantum dots is enhanced with increased quantum confinement (decrease in the size of QDs) since the confinement effect causes an increase in the number of surface states thereby resulting to more holes and electrons to be accessible for the TL recombination (Pagonis *et al*., 2006). Besides, as a consequence extreme confinement the wave functions of the electrons and holes in the QDs are

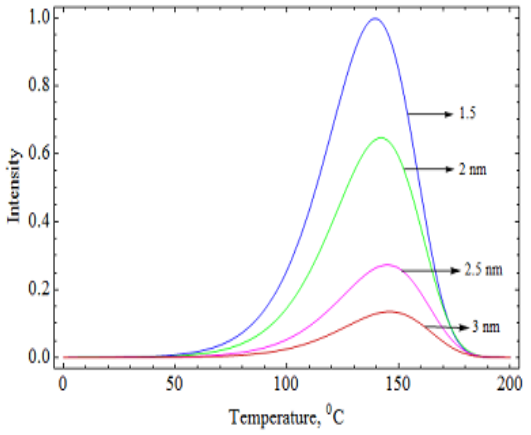

Figure 5: The normalized TL intensity versus temperature for different quantum dot sizes. The parameters are the same as that in Figure 2.

overlapped effectively, resulting in an increase of their radiative recombination rates (Abdul-Ameer and Abdulrida, 2011).

Furthermore, the shape (geometrical) properties of the peaks as well as relevant TL parameters are determined as depicted in Table 2. The widths of the glow curve almost remains constant independent of the size of the dots, i.e., $\omega = T_2 - T_1 \approx 47\ ^0C$. For all QDs size, the TL glow curves have asymmetrical shapes corresponding to first-order 'looking' glow curve with $\mu_g \to 0.42$ and order of kinetics, $b \to 1$; in agreement with that reported in Ref. 3 (Belayneh and Teshome, 2019). This is mainly attributed to the large number of electrons in the TDDTs (Ankama *et al*, 2011). Also, comparison of Figures 4 and 5 shows that the simulated TL glow curve has a very similar shape and the same peak temperature as that of the concentration of electrons in the conduction band.

Table 2. The peak temperature T_m, symmetry factor μ_g, and order of kinetics b for each computed glow curve of different QDs size (IMTS model).

$r\,(nm)$	$T_m\,(K)$	$\omega(K)$	$\delta(K)$	$\mu_g = \delta/\omega$	b
1.5	413.0	46.3	19.7	0.425	1.096
2.0	415.4	47.4	20.1	0.424	1.088
2.5	417.9	46.5	19.7	0.424	1.088
3.0	419.1	46.9	19.6	0.418	1.044

Next, we considered the case for which the TDDT trap is absent. Therefore, setting $M = m_0 = 0$ or equivalently $A_m = 0$ in Eqs. (1) - (5), the IMTS model reduces to the simple one-trap-one-recombination-center (OTOR) model. Figure 6 depicts the intensity of the TL glow curves due to the OTOR model as a function of temperature for the same QDs sizes as that used for the IMTS model. The intensity of the TL emission is found to increase with a decrease of the quantum dots sizes, while the peak temperatures shift towards higher values with an increase in the QDs size; in agreement with Refs. 3, 9, and 10.

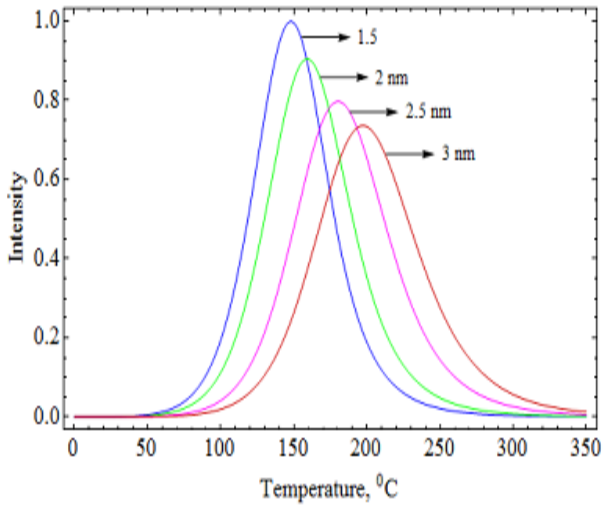

Figure 6: The normalized TL intensity versus temperature for different quantum dot sizes using the OTOR model. Here, $M = m_0 = 0$ while the other parameters are the same as that in Figure 2.

In addition, the shape properties of the glow curves are determined and displayed in Table 3. It is seen that the widths (ω) at half-maxima of the glow curves become broader and broader with an increase in the QDs size. Also, unlike that obtained using the IMTS model, the TL glow curves possess almost symmetrical shapes showing that the OTOR model results to second-order 'looking' glow peaks with $\mu_g \to 0.52$ and $b \to 2$. This is because that in the absence of the TDDT traps, the occurrence of second-order kinetics requires that the electron trap (in our case $n_0 / N = 0.02$) is far from being saturated (Karmakar *et al*., 2017).

Table 3. The peak temperature T_m, symmetry factor μ_g, and order of kinetics b for each computed glow curve of different QDs size (OTOR model).

$r\,(nm)$	$T_m\,(K)$	$\omega(K)$	$\delta(K)$	$\mu_g = \delta/\omega$	b
1.5	421.1	59.5	30.0	0.504	1.770
2.0	432.3	66.5	33.9	0.510	1.830
2.5	453.2	74.6	39.2	0.525	1.898
3.0	470.8	81.7	42.2	0.519	1.924

Lastly, it is worth noting that the OTOR model with $A_n / A_h < 1$, which in our case ranges between 0.03 - 0.50, is expected to result in a second-order glow curve (Pagonis *et al*., 2006). However, the introduction of the thermally disconnected deep traps in the OTOR model changes completely the scenario, i.e., the corresponding IMTS (OTOR + TDDT) model results in first-order kinetics as shown in Figure 5.

CONCLUSIONS

Employing the IMTS TL kinetic model, we investigated the TL glow curves and determine relevant parameters of interest of TL emission from a-Si QDs having different sizes. We find that as the size of the QDs decrease, the intensity of the TL signal is enhanced. Furthermore, for the same QDs, the TL intensity as a function of the size of the QDs is simulated using the OTOR model, i.e., by setting $M = m_0 = 0$ in the IMTS kinetic equations. Similar to that obtained using the IMTS, the intensity of the TL emission is found to increase, with a decrease in the size of the dots. These enhancements of the intensity of TL signal with a decrease in the QDs sizes may be attributed to the quantum confinement effect in nanostructured materials. Furthermore, our analysis shows that irrespective of the presence of retrapping, the glow curves for the IMTS model obey first-order kinetics, while that for the OTOR model obey second-order kinetics. On the other hand, with an increase in the QDs size the peak temperatures shift toward higher values for the OTOR model, unlike that for the IMTS model which are almost independent of size. In addition, the instantaneous concentration of the carriers in the electron traps, conduction band, and RC are determined. We believe that the results may be used during the design and fabrication of dielectric compounds enriched in different ways with silicon contents for TL applications. Further, it may motivate further theoretical and experimental study of the TL phenomena in silicon quantum dots.

ACKNOWLEDGEMENTS

The authors would like to express their gratitude to the Department of Physics of the Addis Ababa University for providing the computational facilities. Asamin Regassa extends his thanks to the Ministry of Education (Ethiopia) for sponsoring his study.

REFERENCES

1. Abdul-Ameer, N.M., and Abdulrida, M.C. (2011).Direct Optical Energy Gap in Amorphous Silicon Quantum Dots. *Journal of Modern Physics*, **2**: 1530–1537.
2. Ankama Rao, K., Niyaz, Sk.P., Poornachandra Rao, N.V., and Murthy, K.V.R. (2011). Thermoluminescence Study of Mineral Ivory Soda. *Archives of Physics Research*, **2(4):**89–93.
3. Belayneh Mesfin and Teshome Senbeta (2019). *Investigation of Size Dependent Thermoluminescence Emission from Amorphous Silicon Quantum Dots,* Bulg. J. Phys., **46:** 37–-48.
4. Cabanas-Tay, S.A., Palacios-Huerta, L., Aceves-Mijares, M., Coyopol, A., Perez-Garcia, S.A., Licea-Jimenez, L., Dominguez, C., and Morales-Sanchez, A. (2016). *Luminescence - An Outlook on the Phenomena and their Applications.*(Ch, 8), INTECH: Open Science, pp. 159–187.
5. Furetta, C. (2003). *Handbook of Thermoluminescence*. World Scientific Publishing Co. Pte. Ltd., Singapore.
6. Karmakar, M., Bhattacharyya, S., Sarkar, A., Mazumdar, P.S., and Singh, S.D. (2017). Analysis of Thermoluminescence Glow Curves using Derivatives of Different Orders. *Radiation Protection Dosimetry*, **175(4):**493–-502.
7. Kwach, H.S., Sun, Y., Cho, Y.H., Park, N.M., and Park, S.J. (2003). Anomalous temperature dependence of optical emission in visible-light-emitting amorphous silicon quantum dots. *Appl. Phys. Lett.*, **83(14):** 2901–2903.
8. Mckeever, S.W.S. (1983). *Thermoluminescence of Solids*. Cambridge University Press, Cambridge.
9. Nebiyu Gemechu, Teshome Senbeta, Belayneh Mesfin, and Mal'nev, V.N. (2017). Thermoluminescence from Silicon Quantum Dots in the Two Traps-One Recombination Center Model. Ukr. J. Phys., **62(2):**140–145.
10. Nebiyu Gemechu, Dejene, F.B., Mal'nev, V.N., Teshome Senbeta, Belayneh Mesfin, and Roroa, K. (2016). Effect of Retrapping on Thermoluminescence Peak Intensities of Small Amorphous Silicon Quantum Dots. *Acta Physica Polonica A*, **129(3):** 362–366.
11. Pagonis, V., and Kitis, G. (2012). Prevalence of first-order kinetics in thermoluminescence materials: An explanation based on multiple competition processes. *Phys. Status Solidi B*, **249(8):** 1590–1601.
12. Pagonis, V., Kitis, G., and Furetta, C. (2006). *Numerical and Practical Exercises in Thermoluminescence*. Springer, New York.
13. Park, N.M., Kim, T.S., and Park, S.J. (2001). Band gap engineering of amorphous silicon quantum dots for light-emitting diodes. *Appl. Phys. Lett.*, **78(17):**2575–-2577.
14. Park, N.M., Choi, C.J., Seong, T.Y., and Park, S.J. (2001). Quantum Confinement in Amorphous Silicon Quantum Dots. *Phys. Rev. Lett.*, **86(7)**: 1355–1357.
15. Rahdar, A., Arbabi, V., and Ghanbari, H. (2012). Study of Electro-Optical Properties of ZnS Nanoparticles Prepared by Colloidal Particles Method. *World Academy of Science: Engineering and Technology*, **61**: 657–659.
16. Rodriguez, J.A., Vasquez-Agustin, M.A., Morales-Sanchez, A., and Aceves-Mijares, M. (2014). Emission Mechanisms of Si Nanocrystals and Defects in SiO_2 Materials. *Jour. of Nanomaterials*, Vol. 2014, Art. ID. 409482.
17. Singh, S.J., Karmakar, M., Bhattacharya, M., Singh, S.D., Singh, W.S., and Azharuddin, S.K. (2012). Modified peak shape method for the determination of activation energy in thermoluminescence. *Ind. J. Phys.*, **86(2)**: 113–-116.
18. Sunta, C. M. (2015). *Unraveling Thermoluminescence*. Springer, New Delhi, India.
19. Takagahara, T., and Takeda, K. (1992). Theory of quantum confinement effect on excitons in quantum dots of indirect-gap materials. *Phys. Rev. B*, **46(23)**: 15578–15581.
20. Tu, C.-C., Zhang, Q., Lin, L.Y., and Cao, G. (2012). Brightly Photoluminescent phosphor materials based on silicon quantum dots with oxide shell passivation. *Optics Express*, **20**(S1): A69–A74.
21. Yoffe, A.D., (1993). Low-dimensional systems: Quantum size effects and electronic properties of semiconductor micro-crystallites (zero-dimensional systems) and some quasi-two-dimensional systems. *Advances in Physics*, **42(2)**: 173–262.